

Pinning down electroweak dipole operators of the top quark

Markus Schulze^{1,*} and Yotam Soreq^{2,†}

¹*CERN Theory Division, 1211 Geneva 23, Switzerland.*

²*Center for Theoretical Physics, Massachusetts Institute of Technology, Cambridge, MA 02139, U.S.A.*

We consider hadronic top quark pair production and pair production in association with a photon or a Z boson to probe electroweak dipole couplings in $t\bar{t}W$, $t\bar{t}\gamma$ and $t\bar{t}Z$ interactions. We demonstrate how measurements of these processes at the 13 TeV LHC can be combined to disentangle and constrain anomalous dipole operators. The construction of cross section ratios allows us to significantly reduce various uncertainties and exploit orthogonal sensitivity between the $t\bar{t}\gamma$ and $t\bar{t}Z$ couplings. In addition, we show that angular correlations in $t\bar{t}$ production can be used to constrain the remaining $t\bar{t}W$ dipole operator. Our approach yields excellent sensitivity to the anomalous couplings and can be a further step towards precise and direct measurements of the top quark electroweak interactions.

I. INTRODUCTION

The dynamics of top quark production and decay have been extensively studied at hadron colliders. Early measurements at the Tevatron have taught us about the production mechanism of heavy quarks pairs in Quantum Chromodynamics (QCD) and later evolved into precision measurements of the top quark mass, spin correlations and the forward-backward asymmetry [1, 2]. Similar measurements have been performed during Run-I of the Large Hadron Collider (LHC) which superseded earlier results at an impressive pace [3, 4]. A myriad of measurements has profoundly shaped our understanding of top physics in the Standard Model (SM) and it led to strong exclusion bounds on new physics.

Despite this progress, our understanding of the electroweak interactions of the top quark (*i.e.* its coupling to electroweak gauge bosons and the Higgs boson) is rather limited. The main reasons are the high production thresholds of the $t\bar{t} + X$ processes, small branching fractions and large backgrounds. First measurements and searches at 7 TeV and 8 TeV LHC have established some of these SM processes [5–13], but detailed studies of electroweak couplings will only be possible with a larger data set at higher energies during Run-II. These studies will certainly improve our understanding of top interactions with the electroweak sector and potentially probe physics beyond the SM.

The flavor-changing $t\bar{t}W$ interaction is the best-known top quark coupling as it is experimentally accessible through top quark decays in $t\bar{t}$ production and single-top quark processes. This is reflected by precise measurements of W helicity fractions and top quark spin correlations [14–17] which can be translated into bounds on anomalous couplings. All other electroweak interactions of the top quark with the Z , γ and the Higgs boson are much less explored. For example, the top quark electric charge, which governs the coupling strength of the vector-

like $t\bar{t}\gamma$ interaction, is known to be $Q_t = +2/3$ with a confidence level larger than 5σ [18–21]. However these determinations were obtained from measuring the electric charges of W boson and b -jet in $t\bar{t}$ production, inferring $Q_t = Q_W + Q_b$. A hard photon was never present in the event sample and the fundamental $t\bar{t}\gamma$ interaction was not probed. Similarly, current LHC data only allows constraints on the vector and axial parts of the $t\bar{t}Z$ vertex with $\mathcal{O}(100\%)$ uncertainties [12], while the respective dipole couplings are unconstrained from hadron collider experiments. We note that low-energy observables, such as rare K and B decays [22–24], together with electroweak precision data [25–28] can provide strong constraints on modified $t\bar{t}Z$ interactions. However, these fairly indirect probes are based on either $Z \rightarrow b\bar{b}$ decays or highly off-shell top quarks and Z bosons in $b \rightarrow s Z^*/\gamma^*$ transitions which rely on additional assumptions on the new physics and are prone to hadronic uncertainties.

This immediately motivates precise studies of the final states $t\bar{t} + Z/\gamma/h$, which yield *direct* sensitivity to the desired couplings. The commencing Run-II of the LHC with a collision energy of 13 TeV will, for the first time, produce sufficiently many events to enable coupling studies. The two final states considered in this paper, $t\bar{t} + \gamma$ and $t\bar{t} + Z(\rightarrow \ell\ell)$, with semi-hadronically decaying top quark pairs, have typical fiducial cross sections of ~ 400 fb and 5 fb, respectively. Hence, we expect about 40,000 $t\bar{t}\gamma$ and 500 $t\bar{t}Z$ events from 100 fb^{-1} of integrated luminosity.

Anomalous electroweak top quark coupling studies using these processes have been presented in Refs. [29–49]. For example, the TopFitter collaboration [45] most recently combined various top quark measurements from the Tevatron and the LHC to present a global fit. In Ref. [36] the authors study dedicated differential observables to probe CP violating top quark decays. Anomalous coupling studies that go beyond the leading-order have been presented in Refs. [37, 42, 44, 46, 47]. In this work, we go beyond previous studies by combining observables from $t\bar{t}$, $t\bar{t} + \gamma$ and $t\bar{t} + Z$ to investigate sensitivity to the three electroweak dipole operators which enter simultaneously in these processes. We construct cross section ratios to cancel correlated uncertainties and investigate angular asymmetries of the top quark decay products to

*Electronic address: markus.schulze@cern.ch

†Electronic address: soreq@mit.edu

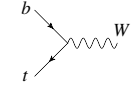
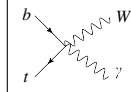
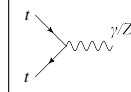
			
C_{uW}^{33}	\otimes	\otimes	\otimes
C_{dW}^{33}	\otimes	\otimes	
$C_{uB\phi}^{33}$			\otimes

Table I: Contribution of dimension-six Wilson coefficients to various vertices appearing in $t\bar{t}$, $t\bar{t} + \gamma$ and $t\bar{t} + Z$ production.

boost sensitivity to possible effects of new physics.

II. SETUP

In the SM, the fundamental interaction vertices of electroweak vector bosons with fermions are given by

$$\Gamma_{q'qV}^{\text{SM}} = \bar{q}' \gamma^\mu (d_L^V P_L + d_R^V P_R) q \varepsilon_\mu^V, \quad (1)$$

where $V = \gamma, Z, W^\pm$ and $P_{L,R}$ are the left and right-handed chirality projectors. The respective couplings $d_{L,R}^V$ are fixed by the quantum numbers and gauge symmetries of the SM, see for example Ref. [50]. In this work, we focus on additional contributions from anomalous electroweak dipole moments in the top quark sector. Their coupling structure is given by

$$\delta\Gamma_{q'qV} = \bar{q}' \frac{i\sigma^{\mu\nu} k_\nu}{m_t} (g_L^V P_L + g_R^V P_R) q \varepsilon_\mu^V, \quad (2)$$

where $\sigma^{\mu\nu} = i/2[\gamma^\mu, \gamma^\nu]$, $k = p_q - p_{q'}$ and $g_{L,R}^V$ are the dipole couplings. The SM has no such interactions at tree level, but electroweak loop corrections radiatively generate dipole moments. Their size is well below 1 per mille [51–53] which makes them inaccessible by LHC experiments. Hence, any sizable deviation from zero will indicate an anomalous interaction from physics beyond the SM. In order to understand how deep the new physics scales can be probed, we investigate the effects of Eq. (2) on physical observables.

Various well-motivated models of new physics [53–59] predict sizable top quark dipole moments. In this work, we adopt a model-independent approach and assume that the new physics is CP conserving and respects the full SM gauge symmetry. We use the effective field theory parameterization of Ref. [50] in terms of higher dimensional operators $\mathcal{L}^{\text{dim6}} = \sum_i C_i/\Lambda^2 \mathcal{O}_i$ and a new physics scale Λ . The relevant operators in our analysis are

$$\mathcal{O}_{uW}^{33} = (\bar{q}_L \sigma^{\mu\nu} \tau^I t_R) \tilde{H} W_{\mu\nu}^I, \quad (3)$$

$$\mathcal{O}_{dW}^{33} = (\bar{q}_L \sigma^{\mu\nu} \tau^I b_R) H W_{\mu\nu}^I, \quad (4)$$

$$\mathcal{O}_{uB\phi}^{33} = (\bar{q}_L \sigma^{\mu\nu} t_R) \tilde{H} B_{\mu\nu}, \quad (5)$$

where $\tilde{H} = i\tau^2 H^*$, $H = (0, h + v)/\sqrt{2}$ is the Higgs boson doublet with the vacuum expectation value $v = 246$ GeV. $B_{\mu\nu}(W_{\mu\nu}^I)$ is the $U(1)_Y(SU(2)_L)$ gauge field

signal strength and I is adjoint $SU(2)_L$ index. $q_L = (t_L, b_L)$, $b_R(t_R)$ are the quark left-handed doublet and bottom (top) right-handed singlet, respectively. Using the parameterization of Eq. (2) and the operators in Eqs. (3)–(5) we find

$$g_L^{W^-} = g_R^{W^{+*}} = -\frac{e m_t}{s_W M_W} \frac{v^2}{\Lambda^2} C_{dW}^{33*}, \quad (6)$$

$$g_R^{W^-} = g_L^{W^{+*}} = -\frac{e m_t}{s_W M_W} \frac{v^2}{\Lambda^2} C_{uW}^{33},$$

$$g_L^\gamma = g_R^{\gamma*} = -\frac{\sqrt{2} m_t v}{\Lambda^2} (c_W C_{uB\phi}^{33*} + s_W C_{uW}^{33*}),$$

$$g_L^Z = g_R^{Z*} = -\frac{e m_t v^2}{\sqrt{2} s_W c_W M_Z \Lambda^2} (c_W C_{uW}^{33*} - s_W C_{uB\phi}^{33*}),$$

where e is the electric coupling and $s_W(c_W)$ is sine (cosine) of the weak mixing angle. We emphasize that since the various dipole couplings in $t\bar{t}W$, $t\bar{t}\gamma/Z$ are related via the underlying $SU(2) \times U(1)$ gauge invariance, the coupling degrees of freedom are reduced to only three Wilson coefficients C_{uW}^{33} , C_{dW}^{33} and $C_{uB\phi}^{33}$. In the expression for $g_{L,R}^{\gamma/Z}$, we see the characteristic weak mixing angle rotation between C_{uW}^{33} and $C_{uB\phi}^{33}$ which will be responsible for the *orthogonal* constraints that we find in $t\bar{t} + \gamma$ and $t\bar{t} + Z$ production below.

At this point we note that there is one more allowed Lorentz-structure in addition to Eq. (2), which is relevant for our analysis,

$$\delta\Gamma_{q'qVV'} = \bar{q}' i\sigma^{\mu\nu} (g_L^{VV'} P_L + g_R^{VV'} P_R) q \varepsilon_\mu^V \varepsilon_\nu^{V'}. \quad (7)$$

This four-point vertex enters our calculation only in one specific place: the radiative top quark decay $t \rightarrow bW + \gamma$ of the $t\bar{t}\gamma$ final state. In a complete description of $t\bar{t}\gamma$ production, the photon can arise from either the hard production stage (*before the top quarks go on-shell*), or the top quark decay stage (*after one top quark went on-shell*). The latter part constitutes more than 50% of the total $t\bar{t}\gamma$ cross section [60] and receives contributions from Eq. (7). It is therefore crucial to account for this contribution in the analysis of $t\bar{t}\gamma$ final states¹. The two additional

¹ The effects from radiative top quark decays are irrelevant for the $t\bar{t} + Z$ process because the decay $t \rightarrow bW + Z$ is suppressed by a phase space factor of 10^{-6} .

dipole couplings in Eq. (7) are given by

$$g_{L,R}^{W^\sigma\gamma} = (-e)\sigma g_{L,R}^{W^\sigma}, \quad (8)$$

where $\sigma = \pm 1$ is the electric charge of the respective W boson. In Table I we summarize the anomalous coefficients considered in our analysis and their appearance in various interaction vertices.

The up-to-date hadron collider bounds on the Wilson coefficients of Eqs. (3–5) are summarized in Ref. [45] and found to be

$$C_{uW}^{33} \in [-4.0, 3.4] (\Lambda/\text{TeV})^2, \quad (9)$$

$$C_{uB\phi}^{33} \in [-7.1, 4.7] (\Lambda/\text{TeV})^2 \quad (10)$$

at 95% confidence level (CL). Note that in order to infer the bound on C_{uW}^{33} , the contributions of all other top-related dimension six operators were marginalized, while for $C_{uB\phi}^{33}$, it was assumed that the only new physics contribution is from $\mathcal{O}_{uB\phi}^{33}$. Finally, in Ref. [32] we find that

$$C_{dW}^{33} \in [-2.3, +2.3] (\Lambda/\text{TeV})^2, \quad (11)$$

at 95% CL. Note that flavor violating contributions from $\mathcal{O}_{uB\phi}^{33}$ can be avoided by alignment to the up sector in flavor space. In that limit, \mathcal{O}_{uW}^{33} induces an irreducible source of flavor violation in the charged current, which is however suppressed by off-diagonal CKM matrix elements, for a more detailed discussion see Ref. [61]. Alignment to the down basis will reduce flavor violation originating from \mathcal{O}_{dW}^{33} , see also the discussion in Ref. [62].

In a strict $1/\Lambda^2$ -expansion within an effective field theory even more operators contribute to the processes considered here. For example, the operator $\bar{\ell}\gamma^\mu\ell\bar{t}\gamma_\mu t$ can enter the $t\bar{t} + Z(\rightarrow \ell\ell)$ process. However, these operators do not exhibit a Breit-Wigner peak structure such as the rest of the amplitude and contribute as a fairly constant function of $m_{\ell\ell}$ around the Z boson mass window of ± 10 GeV, see e.g. Fig. 5 in [38]. Hence, their interference at $\mathcal{O}(\Lambda^{-2})$ integrates to zero and only their squared contribution at $\mathcal{O}(\Lambda^{-4})$ survives. We therefore neglect all operators with fermionic contact interactions. Potential contributions from chromo-magnetic and chromo-electric dipole moments can enter our processes through anomalous top-gluon couplings. However, in this work, we assume that QCD is unaltered by new physics and we do not consider chromo-dipole moments. If QCD is truly non-fundamental, these anomalous interactions are best searched for in jet processes, $gg \rightarrow H$ or $t\bar{t}$ production, see e.g. Ref. [63].

Besides dipole interactions, also the strength of the $t\bar{t}Z$ and $t\bar{t}W$ vector and axial couplings can be altered by new physics. In this work we assume their SM value which is a restrictive assumption on new physics scenarios. Let us therefore comment on possible strategies for a broader analysis in future extensions of our work. One straight-forward solution is to consider

the full space of couplings in a 6-dimensional analysis (anomalous vector and axial-vector couplings introduce three more operators to the ones considered here [50]). This approach might however be challenging given the large number of degrees of freedom and the limited number of events. Another solution may be a careful analysis of kinematics in sequential steps: (i) A first analysis of the process $pp \rightarrow t\bar{t} + \gamma$ can yield information on the dipole moments. Anomalous vector or axial-vector couplings cannot develop thanks to gauge symmetries. (ii) Any deviation in $t\bar{t} + \gamma$ immediately predicts anomalies in the $pp \rightarrow t\bar{t} + Z$ process, as can be seen from Eq. (6). In Ref. [44] it has been shown that dipole couplings most prominently manifest in energy related contributions such as $p_{T,Z}$. Hence, any remaining discrepancy from anomalous vector and axial-vector couplings can be detected in angular distributions, such as $\Delta\phi_{\ell\ell}$, which are sufficiently independent of energies. (iii) Once anomalous dipole couplings in $t\bar{t} + \gamma/Z$ are established, only one remaining dipole operators in $t\bar{t}W$ interactions remains and can be constrained as outlined in Sect. IV. Additional anomalous vector and axial couplings in the $t\bar{t}W$ interaction can then be constrained by relating analyses of top quark pair and single-top quark production $qb \rightarrow W \rightarrow q't$ [32]. Finally, we note that scenarios of large CP-violating electric dipole moments have been extensively studied in the literature [54, 56, 64–66]. These effects arise through CP violation in loop contributions and we expect them to similarly affect the magnetic dipole moments.

Our description of the processes $t\bar{t}$, $t\bar{t} + \gamma$ and $t\bar{t} + Z(\rightarrow \ell\ell)$ treats top quarks in the narrow-width approximation and includes the full decay chain of the top quarks into a single lepton plus jets final state. All spin-correlations are retained. In $t\bar{t} + \gamma$ final states, the photon is allowed to be emitted in the top quark production stage as well as in the decay stage (including the W and W decay products). The Monte Carlo simulation is based on the TOPAZ code [67] developed in Refs. [42, 44, 68], which we extended to handle all anomalous couplings needed in this analysis. If not otherwise stated, we use the following generic selection cuts for the $t\bar{t}$, $t\bar{t} + \gamma$ and $t\bar{t} + Z$ processes

$$\begin{aligned} p_{\perp}^{\ell} &\geq 20 \text{ GeV}, & |y_{\ell}| &\leq 2.5, & E_{\perp}^{\text{miss}} &\geq 20 \text{ GeV}, \\ p_{\perp}^{j,b} &\geq 20 \text{ GeV}, & |y_j| &\leq 2.5, & |y_b| &\leq 2.0. \end{aligned} \quad (12)$$

Jets are defined by the anti- k_T jet algorithm [69] with $R = 0.4$. In addition, for $t\bar{t} + Z$ production we require an invariant mass cut of $|m_{\ell\ell} - M_Z| \leq 10$ GeV. For $t\bar{t} + \gamma$ we require the isolation cuts $R_{\gamma j} = R_{\gamma\ell} = 0.4$ for photons with $p_{\perp}^{\gamma} \geq p_{\perp}^{\gamma, \text{cut}} = 20$ GeV and $|y_{\gamma}| \leq 2.5$. In accordance with the findings at NLO QCD [44, 60], we set the central renormalization and factorization scales to $\mu = m_t$ for $t\bar{t}$ and $t\bar{t} + \gamma$ production, and $\mu = m_t + M_Z/2$ for $t\bar{t} + Z$ production. We use NNPDF3.0 [70] parton distribution functions, $m_t = 173.2$ GeV, $M_Z = 91.1876$ GeV, $M_W = 80.399$ GeV, $G_F = 1.16639 \times 10^{-5}$ GeV $^{-2}$, and use $\alpha = 1/137$ in the $t\bar{t}\gamma$ process.

III. CROSS SECTION RATIOS

In the following we study the sensitivity of different cross section ratios to the anomalous dipole couplings. Ratios of observables have the advantage that leading uncertainties on e.g. α_s and parton distribution functions (PDFs) largely cancel. Even higher order corrections are expected to cancel to some extent, provided that the cross sections are probed in similar regions of phase space. Experimental uncertainties related to luminosity and jet energy scales drop out in the ratio, as well.

A similar idea of employing ratios has been presented in Ref. [71] for measuring the top quark Yukawa coupling at the 100 TeV Future Circular Collider. The authors consider the cross section ratio of $t\bar{t} + H$ over $t\bar{t} + Z$ and demonstrate that a precision of 1% can be reached. This certainly extreme precision is obtained thanks to the kinematic similarities of the two processes and the enormous event rate at a 100 TeV collider. Hence, in the context of this work it seems suggestive to study the ratio $\sigma_{t\bar{t}Z}/\sigma_{t\bar{t}\gamma}$. Yet, we refrain from doing so and instead construct two ratios

$$\mathcal{R}_\gamma = \sigma_{t\bar{t}\gamma}/\sigma_{t\bar{t}}, \quad \mathcal{R}_Z = \sigma_{t\bar{t}Z}/\sigma_{t\bar{t}}, \quad (13)$$

with respect to the $t\bar{t}$ cross section. This allows to benefit from the large $\sigma_{t\bar{t}}$ cross section which has almost no statistical uncertainties. Moreover, we will find that $\sigma_{t\bar{t}Z}$ and $\sigma_{t\bar{t}\gamma}$ have orthogonal dependence on the anomalous couplings which is distinctly exposed in the ratios of Eq. (13). Of course, it is no longer given that uncertainties cancel in these ratios because the $t\bar{t} + \gamma/Z$ and $t\bar{t}$ processes probe very different energies and phase spaces. For example, using the cuts in Eq. (12) we find at leading order an average center-of-mass energy of $\langle \hat{E} \rangle \approx 525$ GeV for the $t\bar{t}$ process, but $\langle \hat{E} \rangle \approx 630$ GeV and 860 GeV for $t\bar{t} + \gamma$ and $t\bar{t} + Z$, respectively. Hence, the parton distribution functions are evaluated at significantly different values of Q^2 and a cancellation of uncertainties is not guaranteed. We circumvent this issue by applying additional (mild) invariant mass cuts on the two $t\bar{t}$ cross sections in Eq. (13) to increase the average center-of-mass energy. In particular, we request $m_{t\bar{t}} \geq 470$ GeV for $\sigma_{t\bar{t}}$ in \mathcal{R}_γ , and $m_{t\bar{t}} \geq 700$ GeV for $\sigma_{t\bar{t}}$ in \mathcal{R}_Z . We verified that the average center-of-mass energy in these two $t\bar{t}$ processes matches the one of the respective $t\bar{t} + \gamma/Z$ process. We note that the experimental reconstruction of the $t\bar{t}$ invariant mass is known to involve large systematic errors. One could therefore worry how this affects the above mentioned cut on $m_{t\bar{t}}$ and how it may spoil the cancellation of uncertainties in the cross section ratios. We therefore investigated variations of this cut and its impact on the ratios \mathcal{R}_γ and \mathcal{R}_Z . While the absolute values obviously change with different values of the cut, we find that our uncertainty estimates presented below are completely unchanged. Even in the extreme case where we remove the $m_{t\bar{t}}$ cuts entirely, our conclusions remain the same as presented below.

To explicitly quantify cancellations of uncertainties in the ratios, we evaluate the cross sections at NLO QCD and study variations of parton distribution functions. This also allows us to obtain error estimates that will be important when estimating sensitivity to the dipole couplings. We partially use results from the NLO QCD computations of $t\bar{t} + \gamma$ and $t\bar{t} + Z$ in Refs. [42, 60] and recompute the NLO $t\bar{t}$ cross sections with the same input parameters and the above mentioned cut on $m_{t\bar{t}}$. The higher average center-of-mass energy of the $t\bar{t}$ cross sections also calls for adapting the renormalization and factorization scales. We find it natural to choose $\mu = m_t + p_{\perp, \text{cut}}^\gamma$ and $\mu = m_t + M_Z/2$ for the two $t\bar{t}$ cross sections in Eq. (13), respectively. Using this setup, we find

$$\mathcal{R}_\gamma^{\text{SM}} \times 10^{-3} = \begin{cases} 11.4_{+0.7\%}^{-0.7\%} & \text{at LO,} \\ 12.6_{-1.8\%}^{+3.1\%} & \text{at NLO QCD,} \end{cases} \quad (14)$$

$$\mathcal{R}_Z^{\text{SM}} \times 10^{-4} = \begin{cases} 2.27_{+2.0\%}^{-1.7\%} & \text{at LO,} \\ 1.99_{+2.8\%}^{-1.9\%} & \text{at NLO QCD.} \end{cases} \quad (15)$$

The upper (lower) values correspond to the lower (upper) scale variation by a factor of two around the respective central scale. We observe a scale dependence of $\pm 1\%$ and $\pm 2\%$ at LO for \mathcal{R}_γ and \mathcal{R}_Z , respectively. These values are slightly increased to $\pm(2-3)\%$ at NLO QCD. This constitutes a remarkable stability with respect to scale variation when compared to the cross sections themselves which exhibit a dependence of about $\pm 20\%$ at NLO. It should be noted that the LO scale variation is far outside the NLO result. This is to be expected as $\alpha_s(\mu_R)$ cancels exactly and the only remaining source of scale dependence arises from unmatched q^2 -dependence in the parton distribution functions. Only our NLO results develop, for the first time, logarithms of the scales with process-dependent coefficients that yield a good error estimate. Hence only the NLO result should be considered a physical meaningful prediction. For our coupling constraints below we will choose the largest value of the NLO scale variation, $\Delta\mathcal{R}_{Z/\gamma} = 3\%$, as our uncertainty for both ratios.

Given the fiducial cross sections of about ~ 5 (400) fb for $t\bar{t}Z$ ($t\bar{t}\gamma$) production, the statistical error is expected to be sub-dominant after an integrated luminosity of about 250 fb^{-1} . This argument is supported by a first measurement of \mathcal{R}_γ by the CMS collaboration [5] at 8 TeV. They find the value $\mathcal{R}_\gamma(8 \text{ TeV}) = 10.7 \times 10^{-3} \pm 6.5\%(\text{stat.}) \pm 25\%(\text{syst.})$ from an integrated luminosity of 19.7 fb^{-1} . The dominant systematics arise from background modeling ($\pm 23\%$) which have the potential to be improved in future analyses.

We also investigate uncertainties from parton distribution functions and find the following results from using

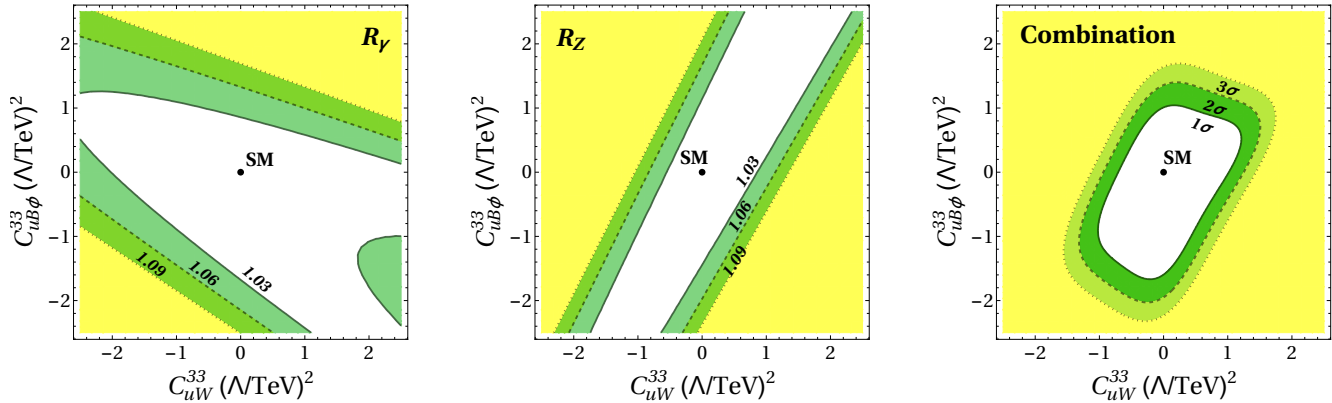


Abbildung 1: Cross section ratios \mathcal{R}_γ (left) and \mathcal{R}_Z (middle) normalized to their SM values ($\mathcal{R}_{\gamma/Z}^{\text{SM}}$) as a function of the anomalous dipole operator couplings. The contours show the deviation from the SM value in steps of 3, 6 and 9 percent. On the right we show the 1, 2, 3 σ contours from combining \mathcal{R}_γ and \mathcal{R}_Z with an assumed uncertainty of $\Delta\mathcal{R}_{Z/\gamma} = 3\%$.

three different sets of parton distribution functions:

$$\mathcal{R}_\gamma^{\text{LO}} \times 10^{-3} = \begin{cases} 11.5 & \text{with NNPDF3.0 [70],} \\ 11.4 & \text{with CTEQ6L1 [72],} \\ 11.5 & \text{with MSTW08 [73],} \end{cases} \quad (16)$$

$$\mathcal{R}_Z^{\text{LO}} \times 10^{-4} = \begin{cases} 2.29 & \text{with NNPDF3.0,} \\ 2.27 & \text{with CTEQ6L1,} \\ 2.27 & \text{with MSTW08.} \end{cases} \quad (17)$$

We observe very stable results with variations at the level of 1%, which have to be compared to $\pm 10\%$ variations on the cross sections themselves. Again, we find confirmation that the ratios are true precision observables.

Finally, let us briefly comment on the impact of electroweak corrections. Compared to the QCD corrections, they are expected to be much less universal for the $t\bar{t}$ and $t\bar{t} + \gamma/Z$ processes. Hence, on the one hand, a cancellation is most likely incomplete. On the other hand, the electroweak corrections on the cross sections are known to be in the few percent range ($\mathcal{O}(\alpha)$) [74, 75]. This leads to a (minor) shift in the absolute values of the ratios but it does not at all affect our estimate of uncertainties.

Let us now turn to studying the effects of anomalous electroweak dipole moments on the cross section ratios. Given two (pseudo-)observables, \mathcal{R}_γ and \mathcal{R}_Z , we investigate their dependence on the Wilson coefficients C_{uW}^{33} and $C_{uB\phi}^{33}$ (neglecting operator mixing and running from beyond the LO). The remaining coefficient C_{dW}^{33} we examine through angular asymmetries in $t\bar{t}$ production in the following section. Since only total cross sections enter this analysis, we are not sensitive to the tail of energy-related distributions where possible issues with unitarity violating EFT operators could appear. We vary the numerical values of C_{uW}^{33} and $C_{uB\phi}^{33}$ between $[-4, 4]$ in steps of 1 and compute 81 LO cross sections for each of

the $t\bar{t}$, $t\bar{t} + \gamma$ and $t\bar{t} + Z$ processes. We then perform a two-dimensional analytic fit of the ratios to present our results. Figure 1 shows the deviation of the anomalous ratios from the SM value for $t\bar{t}\gamma$ on the left and $t\bar{t}Z$ in the middle. These two plots strikingly show the *orthogonal* dependence of the two ratios on the dipole couplings. This is a consequence of the already mentioned s_W rotation pattern of $g_{L,R}^{\gamma,Z}$ in Eq. (6). The white (dark green) bands in left and middle plot of Fig. 1 indicate the parameter spaces where the anomalous cross section ratios deviate from the SM by less than the assumed 1 (2) standard deviation of the assumed uncertainty. Hence, all anomalous couplings outside the dark green bands can be excluded if the measurement is in agreement with the SM at the 2 σ level. In the third plot, on the right of Fig. 1, we show the combination of the two constraints using a naive χ^2 combination. This noticeably leads to a striking improvement of the constraints as the *orthogonal* dependence on the Wilson coefficients allows us to completely bound the parameter space without a blind direction. We note that these projected bounds are stronger by factors of 2-3 compared to the current bounds from 7 and 8 TeV cross section measurements. Moreover, a better understanding of the anomalous $pp \rightarrow b\bar{b}l\nu jj + \gamma$ process beyond the LO will further improve these results. Such a calculation is currently not available and we refer to future work.

IV. ANGULAR ASYMMETRIES IN $t\bar{t}$ PRODUCTION

In this section we expand and complement the constraints obtained from $t\bar{t} + \gamma$ and $t\bar{t} + Z$ in the previous section. We make use of large $t\bar{t}$ cross section at the LHC to define asymmetries of angular distributions from the top quark decay products in order to constrain the remaining Wilson coefficient C_{dW}^{33} , and to over-constrain

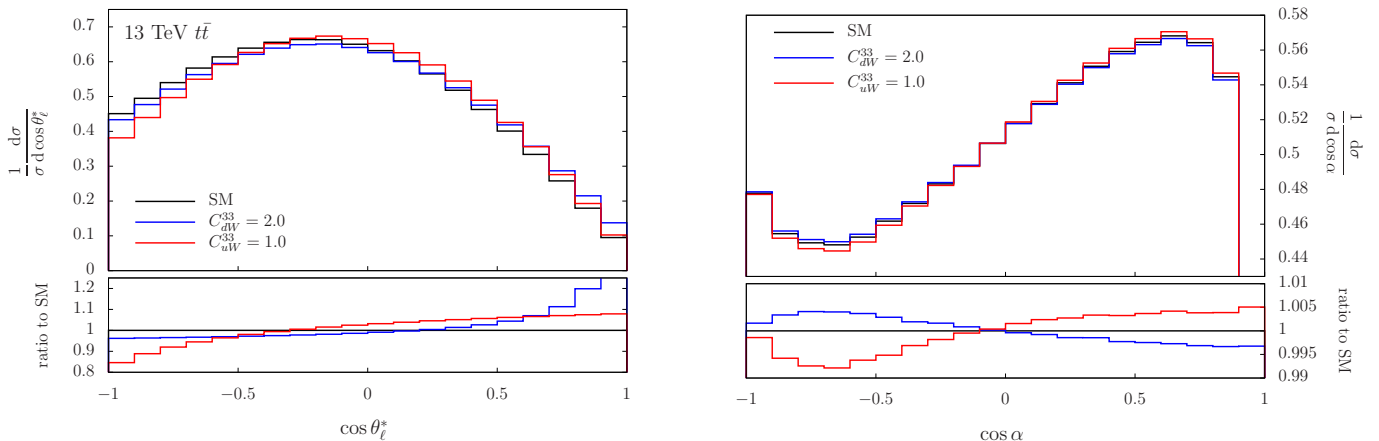


Abbildung 2: Angular distributions in $pp \rightarrow t\bar{t} \rightarrow b\bar{b} l\nu jj$ at 13 TeV used to construct the asymmetries $A_{\theta_\ell^*}$ and A_α .

C_{uW}^{33} . As before, we use the lepton+jet final state of the $t\bar{t}$ system. Similar ideas have been presented in Ref. [31], which puts more emphasis on probing the complex phases of the anomalous couplings. Here, we consider the two angles, defined by

$$\cos \theta_\ell^* = \frac{\vec{p}_\ell \cdot \vec{p}_W}{|\vec{p}_\ell| |\vec{p}_W|}, \quad \cos \alpha = \frac{\vec{p}_t \cdot \vec{p}_W}{|\vec{p}_t| |\vec{p}_W|}, \quad (18)$$

where \vec{p}_ℓ is the lepton momentum in the corresponding W rest frame, \vec{p}_W is the W momentum in the corresponding top quark rest frame, and \vec{p}_t is the top quark momentum in the laboratory frame. Their kinematic distributions are shown in Fig. 2 for the SM and two anomalous coupling choices. From these distributions we construct asymmetries

$$A_\phi(c_0) = \frac{\sigma(\cos \phi < c_0) - \sigma(\cos \phi > c_0)}{\sigma(\cos \phi < c_0) + \sigma(\cos \phi > c_0)}, \quad (19)$$

and use $A_{\theta_\ell^*}(-0.1)$ and $A_\alpha(0.0)$ to maximize their value in our analysis. We evaluated the SM asymmetries at NLO QCD and find perturbative shifts of only $\mathcal{O}(+0.5\%)$. In our coupling analysis below we will assume a slightly inflated uncertainty of $\pm 4\%$. On the experimental side, we expect a similar precision because of the large statistical sample at 13 TeV and the fact that existing measurements at 8 TeV already reach 10% precision for spin asymmetries [76, 77].

To probe the sensitivity of the two asymmetries to the dipole couplings we vary C_{dW}^{33} and C_{uW}^{33} between $[-4, 4]$ in steps of 0.5. Hence, we perform 324 computations at leading order and sub-sequentially fit the results to an analytic parameterization that is shown in Fig. 3. Interestingly, the functional dependence of the asymmetries on the dipole operator couplings is opposite: $A_{\theta_\ell^*}$ has a concave shape (Fig. 3, left) as a function of C_{uW}^{33} and C_{dW}^{33} , whereas A_α (middle) is convexly shaped. This feature allows us to combine the two constraints, shown on the right of Fig. 3, in order to break the (white) invariance

bands of the two separate observables. As a result, both anomalous operators are clearly bounded in the combination plot. Moreover, the constraints on C_{uW}^{33} can be further utilized in conjunction with the bounds obtained from cross section ratios (Fig. 1, right) as they exclude almost the entire region of positive C_{uW}^{33} values. Turning the argument around, two independent measurements of 1) cross section ratios and 2) angular asymmetries can also be used to over-constrain the Wilson coefficient C_{uW}^{33} .

V. SUMMARY

In this paper we investigated the prospects of constraining electroweak dipole moments of the top quark at the 13 TeV LHC. The SM radiatively generates these couplings through electroweak loop corrections, which turn out to be too small to be observed at the LHC. This opens up the possibility to search for sizable deviations from zero as a way to probe new physics in the top quark sector.

We considered all anomalous dipole interactions between the top quark and the electroweak gauge bosons in $t\bar{t}W$, $t\bar{t}\gamma$ and $t\bar{t}Z$ interactions, and we showed that the processes $pp \rightarrow t\bar{t}$ and $pp \rightarrow t\bar{t} + \gamma/Z$ are ideal probes for studying them. While these couplings enter simultaneously in various places, electroweak gauge symmetries relate them and lead to only a small number of relevant operators. In order to constrain and disentangle them, we propose the study of cross section ratios to make use of *orthogonal* sensitivity to anomalous operators entering $t\bar{t}\gamma$ and $t\bar{t}Z$. We carefully investigated the ratios at NLO QCD and verify a strong reduction of uncertainties related to parton distribution functions and higher-order corrections. Experimental systematics such as luminosity or jet energy scale uncertainties are expected to drop out as well, yielding true precision observables.

The final results of our study confirm this picture as we find that 13 TeV data can place firm bounds on the contributing operators. Marginalizing over other operators,

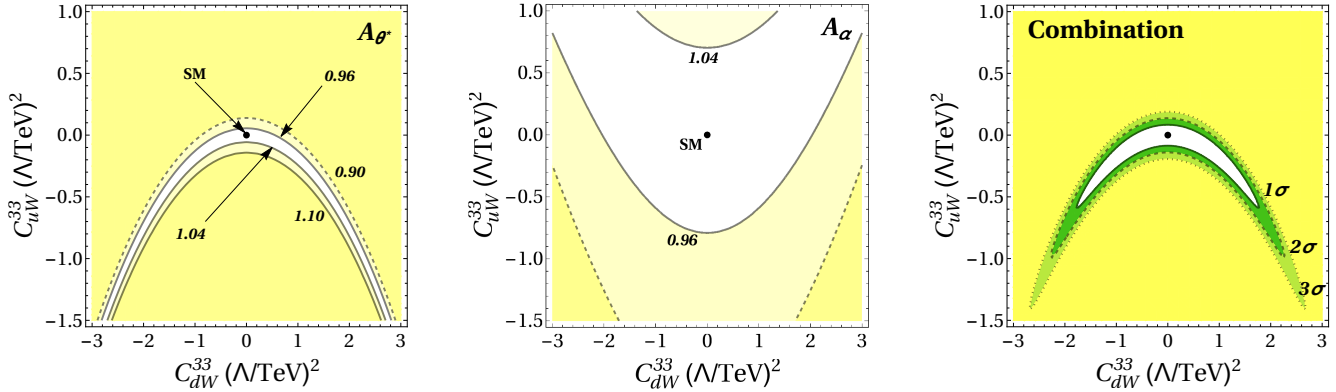


Abbildung 3: Angular asymmetries $A_{\theta_\ell^*}(-0.1)$ (left) and $A_\alpha(0.0)$ (middle) as a function of the two Wilson coefficients in $t\bar{t}$ production relative to their SM values. Right: χ^2 combination of the two asymmetries assuming an uncertainty of $\pm 4\%$.

we find sensitivity of $C_{uW}^{33} = [-1.2, +1.4] (\Lambda/\text{TeV})^2$ and $C_{uB\phi}^{33} = [-1.9, +1.2] (\Lambda/\text{TeV})^2$ at the 95% CL from combining the cross section ratios, assuming that the theoretical accuracy of 3% is matched by the experimental one.

We corroborate our results by studying angular asymmetries in $t\bar{t}$ production to bound the last operator in our analysis and find the sensitivity $C_{dW}^{33} = [-2.0, +2.0] (\Lambda/\text{TeV})^2$. Since the angular asymmetries are also sensitive to C_{uW}^{33} , they can yield the independent constraint $C_{uW}^{33} = [-0.8, +0.1] (\Lambda/\text{TeV})^2$ which can be further used to boost our results from cross section ratios. Altogether, our proposal to construct four precision observables allows to pin down all of the three anomalous electroweak dipole operators without a blind direction.

We note that for a 100 TeV pp collider the $t\bar{t}Z$ and $t\bar{t}\gamma$ cross sections are about a factor of 30 larger than at the 13 TeV LHC. Thus, the statistical error will be subdominant only after a few tens fb^{-1} of integrated luminosity. In order to fully exploit the potential of a 1 ab^{-1} data set, the theoretical predictions should be improved by one order of magnitude. Theoretical control of cross section ratios at the per-mille level may be possible on-

ce predictions at next-to-next-to-leading order QCD are available for $t\bar{t} + \gamma/Z$. This does not seem unrealistic on the relevant time scale and would boost the constraints by more than 100%.

Future work on improving our results could be a more precise understanding of uncertainties of the cross section ratios. For example, it would be desirable to have the complete NLO predictions for the $t\bar{t} + \gamma$ process with anomalous couplings. A fully realistic analysis also needs to consider backgrounds which we neglected in this work. The incorporation of single-top quark processes into our analysis or more differential observables will certainly further strengthen sensitivity to new physics.

Acknowledgments

We thank Michelangelo Mangano, Gilad Perez, Raoul Röntsch for comments on the manuscript and Jesse Thaler for helpful discussions. M.S. is grateful for the hospitality at MIT-CTP where this project was initiated. Y.S. is supported by the U.S. Department of Energy (DOE) under cooperative research agreement DE-SC-00012567.

-
- [1] D. Wicke, Eur. Phys. J. **C71**, 1627 (2011), 1005.2460.
 - [2] F. Deliot and D. A. Glazinski, Rev. Mod. Phys. **84**, 211 (2012), 1010.1202.
 - [3] F.-P. Schilling, Int. J. Mod. Phys. **A27**, 1230016 (2012), 1206.4484.
 - [4] V. del Duca and E. Laenen, Int. J. Mod. Phys. **A30**, 1530063 (2015), 1510.06690.
 - [5] V. Khachatryan et al. (CMS), CMS-PAS-TOP-13-011 (2014).
 - [6] V. Khachatryan et al. (CMS), JHEP **09**, 087 (2014), [Erratum: JHEP10,106(2014)], 1408.1682.
 - [7] G. Aad et al. (ATLAS), Phys. Lett. **B749**, 519 (2015), 1506.05988.
 - [8] G. Aad et al. (ATLAS), Eur. Phys. J. **C75**, 349 (2015), 1503.05066.
 - [9] G. Aad et al. (ATLAS), Phys. Lett. **B740**, 222 (2015), 1409.3122.
 - [10] G. Aad et al. (ATLAS), Phys. Rev. **D91**, 072007 (2015), 1502.00586.
 - [11] V. Khachatryan et al. (CMS), Eur. Phys. J. **C75**, 251 (2015), 1502.02485.
 - [12] V. Khachatryan et al. (CMS), JHEP **01**, 096 (2016), 1510.01131.
 - [13] G. Aad et al. (ATLAS), JHEP **11**, 172 (2015), 1509.05276.
 - [14] T. Aaltonen et al. (CDF, D0), Phys. Rev. **D85**, 071106

- (2012), 1202.5272.
- [15] V. Khachatryan et al. (CMS), JHEP **01**, 053 (2015), 1410.1154.
- [16] G. Aad et al. (ATLAS), Phys. Rev. **D93**, 012002 (2016), 1510.07478.
- [17] G. Aad et al. (ATLAS) (2015), 1510.03764.
- [18] G. Aad et al. (ATLAS), ATLAS-CONF-2011-141 (2011).
- [19] V. Khachatryan et al. (CMS), CMS-PAS-TOP-11-031 (2012).
- [20] T. Aaltonen et al. (CDF), Phys. Rev. **D88**, 032003 (2013), 1304.4141.
- [21] V. M. Abazov et al. (D0), Phys. Rev. **D90**, 051101 (2014), [Erratum: Phys. Rev.D90,no.7,079904(2014)], 1407.4837.
- [22] B. Grzadkowski and M. Misiak, Phys. Rev. **D78**, 077501 (2008), [Erratum: Phys. Rev.D84,059903(2011)], 0802.1413.
- [23] J. F. Kamenik, M. Papucci, and A. Weiler, Phys. Rev. **D85**, 071501 (2012), [Erratum: Phys. Rev.D88,no.3,039903(2013)], 1107.3143.
- [24] J. Brod, A. Greljo, E. Stamou, and P. Uttayararat, JHEP **02**, 141 (2015), 1408.0792.
- [25] S. Schael et al. (SLD Electroweak Group, DELPHI, ALEPH, SLD, SLD Heavy Flavour Group, OPAL, LEP Electroweak Working Group, L3), Phys. Rept. **427**, 257 (2006), hep-ex/0509008.
- [26] J. Abdallah et al. (DELPHI), Eur. Phys. J. **C60**, 1 (2009), 0901.4461.
- [27] F. Larios, M. A. Perez, and C. P. Yuan, Phys. Lett. **B457**, 334 (1999), hep-ph/9903394.
- [28] J. de Blas, M. Chala, and J. Santiago, JHEP **09**, 189 (2015), 1507.00757.
- [29] U. Baur, A. Juste, L. H. Orr, and D. Rainwater, Phys. Rev. **D71**, 054013 (2005), hep-ph/0412021.
- [30] E. L. Berger, Q.-H. Cao, and I. Low, Phys. Rev. **D80**, 074020 (2009), 0907.2191.
- [31] J. A. Aguilar-Saavedra and J. Bernabeu, Nucl. Phys. **B840**, 349 (2010), 1005.5382.
- [32] J. A. Aguilar-Saavedra, N. F. Castro, and A. Onofre, Phys. Rev. **D83**, 117301 (2011), 1105.0117.
- [33] S. D. Rindani and P. Sharma, JHEP **11**, 082 (2011), 1107.2597.
- [34] F. Bach and T. Ohl, Phys. Rev. **D86**, 114026 (2012), 1209.4564.
- [35] C. Zhang, N. Greiner, and S. Willenbrock, Phys. Rev. **D86**, 014024 (2012), 1201.6670.
- [36] J. A. Aguilar-Saavedra and S. A. dos Santos, Phys. Rev. **D89**, 114009 (2014), 1404.1585.
- [37] C. Zhang, Phys. Rev. **D90**, 014008 (2014), 1404.1264.
- [38] G. Durieux, F. Maltoni, and C. Zhang, Phys. Rev. **D91**, 074017 (2015), 1412.7166.
- [39] A. Prasath V, R. M. Godbole, and S. D. Rindani, Eur. Phys. J. **C75**, 402 (2015), 1405.1264.
- [40] J. A. Aguilar-Saavedra, E. Alvarez, A. Juste, and F. Rubbo, JHEP **04**, 188 (2014), 1402.3598.
- [41] C. Bernardo, N. F. Castro, M. C. N. Fiolhais, H. Goncalves, A. G. C. Guerra, M. Oliveira, and A. Onofre, Phys. Rev. **D90**, 113007 (2014), 1408.7063.
- [42] R. Rontsch and M. Schulze, JHEP **07**, 091 (2014), [Erratum: JHEP09,132(2015)], 1404.1005.
- [43] A. Tonerio and R. Rosenfeld, Phys. Rev. **D90**, 017701 (2014), 1404.2581.
- [44] R. Rontsch and M. Schulze, JHEP **08**, 044 (2015), 1501.05939.
- [45] A. Buckley, C. Englert, J. Ferrando, D. J. Miller, L. Moore, M. Russell, and C. D. White (2015), 1512.03360.
- [46] C. Zhang (2016), 1601.06163.
- [47] O. B. Bylund, F. Maltoni, I. Tsinikos, E. Vryonidou, and C. Zhang (2016), 1601.08193.
- [48] Q.-H. Cao, B. Yan, J.-H. Yu, and C. Zhang (2015), 1504.03785.
- [49] V. Cirigliano, W. Dekens, J. de Vries, and E. Mereghetti (2016), 1603.03049.
- [50] J. A. Aguilar-Saavedra, Nucl. Phys. **B812**, 181 (2009), 0811.3842.
- [51] J. Bernabeu, D. Comelli, L. Lavoura, and J. P. Silva, Phys. Rev. **D53**, 5222 (1996), hep-ph/9509416.
- [52] A. Czarnecki and B. Krause, Acta Phys. Polon. **B28**, 829 (1997), hep-ph/9611299.
- [53] W. Hollik, J. I. Illana, S. Rigolin, C. Schappacher, and D. Stockinger, Nucl. Phys. **B551**, 3 (1999), [Erratum: Nucl. Phys.B557,407(1999)], hep-ph/9812298.
- [54] K. Agashe, G. Perez, and A. Soni, Phys. Rev. **D75**, 015002 (2007), hep-ph/0606293.
- [55] A. L. Kagan, G. Perez, T. Volansky, and J. Zupan, Phys. Rev. **D80**, 076002 (2009), 0903.1794.
- [56] T. Ibrahim and P. Nath, Phys. Rev. **D82**, 055001 (2010), 1007.0432.
- [57] T. Ibrahim and P. Nath, Phys. Rev. **D84**, 015003 (2011), 1104.3851.
- [58] C. Grojean, O. Matsedonskyi, and G. Panico, JHEP **10**, 160 (2013), 1306.4655.
- [59] F. Richard (2013), 1304.3594.
- [60] K. Melnikov, M. Schulze, and A. Scharf, Phys. Rev. **D83**, 074013 (2011), 1102.1967.
- [61] P. J. Fox, Z. Ligeti, M. Papucci, G. Perez, and M. D. Schwartz, Phys. Rev. **D78**, 054008 (2008), 0704.1482.
- [62] J. Drobnak, S. Fajfer, and J. F. Kamenik, Nucl. Phys. **B855**, 82 (2012), 1109.2357.
- [63] J. A. Aguilar-Saavedra, B. Fuks, and M. L. Mangano, Phys. Rev. **D91**, 094021 (2015), 1412.6654.
- [64] W. Bernreuther, T. Schroder, and T. N. Pham, Phys. Lett. **B279**, 389 (1992).
- [65] J. Hernandez-Sanchez, F. Procopio, G. Tavares-Velasco, and J. J. Toscano, Phys. Rev. **D75**, 073017 (2007), hep-ph/0611379.
- [66] W. Dekens, J. de Vries, J. Bsaisou, W. Bernreuther, C. Hanhart, U.-G. Meißner, A. Nogga, and A. Wirzba, JHEP **07**, 069 (2014), 1404.6082.
- [67] M. Schulze and R. Röntsch, *Topaz*, <https://github.com/TOPAZdevelop/TOPAZ> (2014).
- [68] K. Melnikov and M. Schulze, JHEP **08**, 049 (2009), 0907.3090.
- [69] M. Cacciari, G. P. Salam, and G. Soyez, JHEP **04**, 063 (2008), 0802.1189.
- [70] R. D. Ball et al. (NNPDF), JHEP **04**, 040 (2015), 1410.8849.
- [71] M. L. Mangano, T. Plehn, P. Reimitz, T. Schell, and H.-S. Shao, J. Phys. **G43**, 035001 (2016), 1507.08169.
- [72] J. Pumplin, D. R. Stump, J. Huston, H. L. Lai, P. M. Nadolsky, and W. K. Tung, JHEP **07**, 012 (2002), hep-ph/0201195.
- [73] A. D. Martin, W. J. Stirling, R. S. Thorne, and G. Watt, Eur. Phys. J. **C63**, 189 (2009), 0901.0002.
- [74] J. H. Kuhn, A. Scharf, and P. Uwer, Phys. Rev. **D91**, 014020 (2015), 1305.5773.
- [75] S. Frixione, V. Hirschi, D. Pagani, H. S. Shao, and M. Zaro, JHEP **06**, 184 (2015), 1504.03446.

[76] V. Khachatryan et al. (CMS) (2016), 1601.01107.

(2015), 1412.4742.

[77] G. Aad et al. (ATLAS), Phys. Rev. Lett. **114**, 142001